Journal of Applied Mechanics and Technical Physics, Vol. 51, No. 4, pp. 529–537, 2010

DYNAMICS OF BOUNDARY LAYER FORMATION IN A VOLCANO CHANNEL IN A CAVITATING HIGH-VISCOSITY MAGMA FLOW

V. K. Kedrinskii and M. N. Davydov

UDC 532.787:550.3

Based on the full mathematical model of a viscous magma melt flow ascending in the gravity field behind a decompression wave front, an unsteady two-dimensional axisymmetric problem of the melt state dynamics at the initial stage of an explosive volcanic eruption and specific features of the flow in the vicinity of the channel wall for the cases of stationary and dynamically increasing viscosity are studied. The evolution of the boundary layer is numerically analyzed for a constant melt viscosity equal to $\mu = 10^3$, 10^5, *and* 10^7 Pa·sec. *It is demonstrated that a boundary layer is formed on the wall of the channel with a radius of* 100 *m as the melt viscosity is changed in the range of* 10^3–10^5 Pa·sec, *and the boundary layer thickness increases from* 2 *to* 15 m. *As the magma viscosity increases to* 10^7 Pa·sec, *the boundary layer chokes the major part of the channel, thus, locking the flow in the vicinity of the axis of symmetry of the channel almost over the entire channel length. Substantial changes in the flow structure caused by dynamically increasing viscosity are demonstrated by an example of the melt in the channel with a radius of* 10 m. *By the time* $t = 1.1$ sec, *the boundary layer thickness in the channel cross section at a height of approximately* 1000 m *reaches almost* 8 m, *the boundary layer acquires the shape similar to a "diaphragm," penetrates inward the channel by* 200 m (*with the mass velocity ranging from* 0 *to* 15 m/sec), *and locks the flow in a zone with a radius of approximately* 2 m *around the axis of symmetry of the channel.*

Key words: *magma melt, mathematical model, viscosity dynamics, boundary layer, channel choking.*

Introduction. Explosive volcanic eruptions involve a wide range of processes developed behind the rarefaction wave front owing to decompression of the magma melt previously compressed to high pressures. The melt state dynamics changes substantially in the course of homogeneous nucleation, diffusion of gases from the melt, and increasing of viscosity by several orders. These processes are directly related to real mechanisms of formation of the flow structure in the volcano channel and actually determine the eruption character and versatile multiscale phenomena accompanying the eruption. The mechanisms of these phenomena are not yet well understood. They include periodicity of explosive ejections observed during eruptions of some volcano types. Numerous physical models were proposed to explain possible mechanisms of these ejections [1]. One of these models describes real processes of bubble coalescence in dense cavitating clusters, which lead to formation of large cavities filled by the gas and magma particles, all compressed to high pressures, in the volcano channel (the so-called "slugs") [2–6]. Possible options are individual "slugs" that occupy almost the entire channel cross sections or a system of "slugs" arbitrarily distributed in the flow [7].

If we assume that periodic ejections are nothing else but results of explosions of these "slugs" [8–10], then their periodicity is determined either by the time necessary for the next "slug" to form or by the time needed for the next nearest "slug" from the system formed in the channel to approach the boundary of the fragmentation region [11]. The following factors are believed to play an important role in possible mechanisms determining

Lavrent'ev Institute of Hydrodynamics, Siberian Division, Russian Academy of Sciences, Novosibirsk 630090; kedr@hydro.nsc.ru. Translated from Prikladnaya Mekhanika i Tekhnicheskaya Fizika, Vol. 51, No. 4, pp. 95–105, July–August, 2010. Original article submitted June 1, 2009.

the ejection periodicity: effects of adhesion and slipping of the high-viscosity magma on the channel walls [12], factors responsible for magma motion (pressure in the magma channel and elasticity of the volcanic channel walls) [13], and variations of the volcanic channel shape over its height [14, 15].

Experimental investigations of the magma state dynamics in the Erebus volcano, which is one of the open volcanic systems, are of much interest [16]. In the depth of the crater of this volcano, there is a lava lake with an open surface, which is assumed to be directly connected to the magma chamber. Approximately 50 explosive eruptions were observed in these experiments at three different observation angles with a system of continuous-emission Doppler radars. The measurements showed that the velocity of cavitating magma ejection exceeds 180 m/sec; gas bubbles in this magma rapidly expand, refrain from oscillations, and explode near the free surface of the lava. This allows us to conclude that the model of periodic ejections in explosive eruptions, which is based on the assumption about the oscillatory character of the dynamics of up-floating bubbles, is inapplicable to strombolian-type volcanoes (with moderate-intensity eruptions), which include the Erebus volcano.

Though viscosity is one of the most important characteristics of the magma melt determining the flow structure, the development of boundary layers on the channel walls was ignored in most investigations of ejection periodicity mechanisms. As direct observations of this process in volcano channels are impossible, mathematical models of mechanics of multiphase media and data on the kinetics of the expected processes become extremely important.

An unsteady two-dimensional axisymmetric problem of the dynamics of the viscous melt state at the initial stage of the volcanic eruption and specific features of the flow near the channel wall in the cases of stationary and dynamically increasing viscosity is studied in the present paper on the basis of the full mathematical model of the ascending magma melt flow in the gravity field with due regard for the processes of nucleation of cavitating bubbles and degassing, dynamics of viscosity growth, and magma crystallization [17].

1. Formulation of the Problem. A cylindrical volcanic channel with rigid walls is partly (up to a height H) filled by a gas-saturated magma (with an initial temperature T_0) containing crystalline nuclei whose volume concentration is $N_{\rm cr}$. The dissolved gas concentration $C^{\rm eq}(p)$ is equal to its equilibrium value and is determined by the Henry law. A constant pressure $p_{\rm ch}$ is set on the lower boundary of the magma column; the pressure in the magma column is distributed in accordance with hydrostatic laws. The upper boundary of the magma column is separated from the atmosphere by a solidified lava plug. At the initial time, the plug is broken, the pressure on the upper boundary decreases to the atmospheric value, and a decompression wave starts to propagate vertically downward the magma column. The melt behind the wave front is in the supersaturated state, which leads to spontaneous nucleation and growth of gas bubbles inside the melt.

The flow of the cavitating magma melt is described by a system of gas-dynamic equations for the mean pressure p, density ρ, and mass velocity components u and v with allowance for variable viscosity in the Navier–Stokes equation:

$$\frac{\partial \rho}{\partial t} + \frac{1}{r}\,\frac{\partial\,(\rho r v)}{\partial r} + \frac{\partial\,(\rho u)}{\partial z} = 0,$$

$$\frac{\partial v}{\partial t} + v\,\frac{\partial v}{\partial r} + u\,\frac{\partial v}{\partial z} = -\frac{\rm Eu}{\rho}\,\frac{\partial p}{\partial r} + \frac{1}{{\rm Re}\,\rho}\Big[\frac{1}{r}\,\frac{\partial}{\partial r}\Big(\mu r\,\frac{\partial v}{\partial r}\Big) + \frac{\partial}{\partial z}\Big(\mu\,\frac{\partial v}{\partial z}\Big) - \frac{v\mu}{r^2}\Big],$$

$$\frac{\partial u}{\partial t} + v\,\frac{\partial u}{\partial r} + u\,\frac{\partial u}{\partial z} = -\frac{\rm Eu}{\rho}\,\frac{\partial p}{\partial z} - \frac{1}{\rm Fr} + \frac{1}{{\rm Re}\,\rho}\Big[\frac{1}{r}\,\frac{\partial}{\partial r}\Big(\mu r\,\frac{\partial u}{\partial r}\Big) + \frac{\partial}{\partial z}\Big(\mu\,\frac{\partial u}{\partial z}\Big)\Big].$$

This system is supplemented with the system of equations [18] determining:

— the state of the mixture and its liquid and gaseous components:

$$\rho = \rho_l(1-k), \qquad p = p_0 + \frac{\rho c^2}{n}\Big[\Big(\frac{\rho}{\rho_0(1-k)}\Big)^n - 1\Big], \qquad \frac{4\pi}{3}\,p_g R^3 = \frac{m_g}{M}\,k_{\rm B};$$

— the kinetics of nucleation and growth of bubbles:

$$k = \frac{\varkappa}{1+\varkappa}, \qquad J = \exp\Big\{-{\rm G}\Big[\Big(\frac{p_{\rm ch}}{\Delta p}\Big)^2 - 1\Big]\Big\},$$

$$R\ddot{R} + \frac{3}{2}\,\dot{R}^2 = \frac{\rm Eu}{\rho}\,(p_g - p) + \frac{4\nu}{\rm Re}\,\frac{\dot{R}}{R},$$

$$\mathrm{Re}\,\mathrm{Pr}_D\,\frac{dm_g}{dt} = 3R(C_i - C^{\mathrm{eq}}(p_g)),$$

$$\varkappa = \frac{4\pi}{3}\,J_0 z_0^3 t_0 \int\limits_0^t J(\tau)R^3(t-\tau)\exp\Big(-\frac{4\pi}{3}\,J_0 z_0^3 t_0(\zeta^3-1)\int\limits_0^\tau J(\tau')R^3(\tau-\tau')\,d\tau'\Big)\,d\tau;$$

— the thermal balance and kinetics of growth of the crystalline mass:

$$\frac{dT}{dt} = \mathrm{Ku}\,\frac{dX}{dt} - \mathrm{Ku}'\,\frac{4\pi}{3}\,N_b z_0^3\,\frac{dm_g}{dt}, \qquad X = \frac{4\pi}{3}\,N_{\mathrm{cr}}\Big(\int\limits_0^t v_{\mathrm{cr}}\,d\tau\Big)^3, \qquad v_{\mathrm{cr}} = \Delta T;$$

— the dependence of medium viscosity on the dissolved gas concentration [19]:

$$\mu = \mu^*\exp\Big(\frac{E_\mu^*(1-k_\mu C)}{k_{\mathrm{B}}T}\Big).$$

In these equations, k is the volume concentration of the gas phase, $\varkappa$ and N_b are the volume fraction of the emerging cavitating nuclei and their density in a unit volume, R is the nucleus radius, p_{ch} is the pressure in the volcanic chamber, J is the frequency of bubble nucleation, C_i is the concentration of the dissolved gas, X is the volume fraction of crystallites, v_{cr} is the growth rate of crystals, $\zeta^3 - 1$ is the relative thickness of the diffusion layer on the cavitating bubble, the subscripts l and g refer to the liquid and gaseous components, respectively, $n = 7$ is the parameter of the Tait equation of state for the liquid component, k_{B} is the Boltzmann constant, M is the molecular weight of the gas, $\nu = \mu/\rho$ is the kinematic viscosity, and τ is the integration variable, σ is the surface tension, D is the coefficient of gas diffusion in the melt, L and r_D are the heats of crystallization and desorption, and c is the heat capacity of the magma; the Euler number $\mathrm{Eu} = p_0/(\rho_0 u_0^2)$, Froude number $\mathrm{Fr} = u_0/(gt_0)$, Reynolds number $\mathrm{Re} = z_0 u_0/\nu_0$, Gibbs number $\mathrm{G} = (16\pi/3)\sigma^3/(p_{\mathrm{ch}}^2 k_{\mathrm{B}}T)$, Prandtl number $\mathrm{Pr}_D = \nu_0/D$, and Kutateladze numbers $\mathrm{Ku} = L/(cT_0)$ and $\mathrm{Ku}' = r_D/(cT_0)$ are the similarity criteria. The system is written in dimensionless variables normalized to their initial values.

The following boundary conditions are imposed: velocity components $v = 0$ and $u = 0$ on the channel wall (no-slip condition), radial component of velocity $v = 0$ on the axis of symmetry, $p = p_0$ and $\partial S/\partial t = \partial(\boldsymbol{v}, \boldsymbol{u})/\partial \boldsymbol{n}$ on the free boundary S, and $p = p_{\mathrm{ch}}$ on the boundary with the magma channel.

2. Results of Modeling. The calculations were performed under the following conditions: initial height of the magma melt column in the volcano channel $H = 1$ km, range of channel radii $R = 10$–100 m, pressure in the volcanic chamber $p_{\mathrm{ch}} = 170$ MPa, temperature $T = 1150$ K, initial density of the magma melt $\rho_0 = 2300$ kg/m^3, and initial mass fraction of the dissolved gas $C_0 = 5\%$. To estimate the probable "ultimate" depth of volcano channel choking by the boundary layer, calculations were also performed for channel radii of 500 and 1000 m. The above-given parameters have the following values: Henry constant $K_{\mathrm{H}} = 4.33 \cdot 10^{-6}$ Pa$^{-1/2}$, $D = 2 \cdot 10^{-11}$ m^2/sec, $\sigma = 0.076$ J/m^2, activation energy of the "dry" melt $E_\mu^* = 5.1 \cdot 10^{-19}$ J, empirical constant $k_\mu = 11$, constant $\mu^* = 10^{-2.5}$ Pa$\cdot$sec, $L = 1.4 \cdot 10^5$ J/kg, $c = 1.35 \cdot 10^3$ J/kg, $N_{\mathrm{cr}} = 10^{12}$ m^{-3}, $\mathrm{Eu} \approx 1$, $\mathrm{Re} \approx 1$, $\mathrm{Fr} \approx 1$, $\mathrm{G} = 16$, and $\mathrm{Pr}_D \approx 10^{11}$.

The flow of the initially motionless magma starts to form behind the front of the decompression wave propagating downward the channel after the diaphragm separating the channel filled by the magma from the free surface is broken. At high values of melt viscosity, the free surface shape is unknown and should be calculated, but the problem of the unknown free surface was skipped at this stage. The free surface was straightened at each time step; the surface was assumed to remain flat and to move with a mass velocity averaged over the cross section. The calculated results are presented in dimensional variables.

In the course of cavitation development behind the decompression wave front, the height H of the examined magma column increases and reaches approximately 1200 m by the time $t = 1.1$ sec. Because of the high viscosity of the medium, the radial component of velocity v in the entire domain is practically equal to zero. Note (according to [20]) that propagation of the rarefaction (decompression) wave in a cavitating medium alters the wave profile: the wave is separated into a precursor propagating with the velocity of sound in the undisturbed medium and the main disturbance propagating with a significantly lower velocity in the two-phase medium. The velocity of the main wave can be reduced by dynamically developing bubble cavitation ahead of its front.

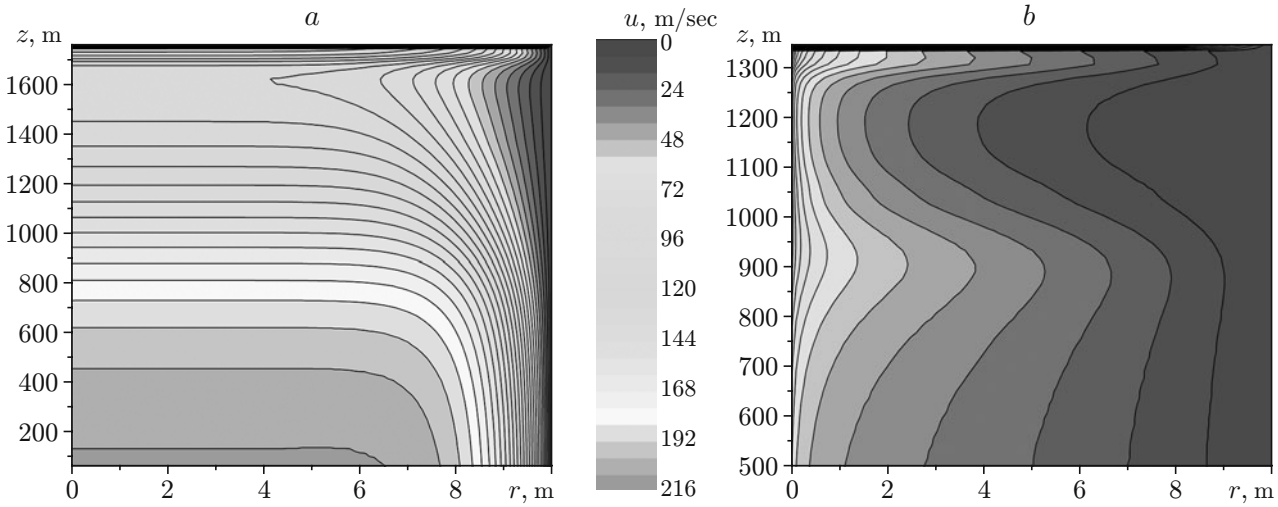

Fig. 1. Profiles of the boundary layers in the channel with the radius of 10 m: (a) $\mu = 10^3$ Pa · sec and $t = 4$ sec; (b) $\mu = 10^5$ Pa · sec and $t = 2$ sec.

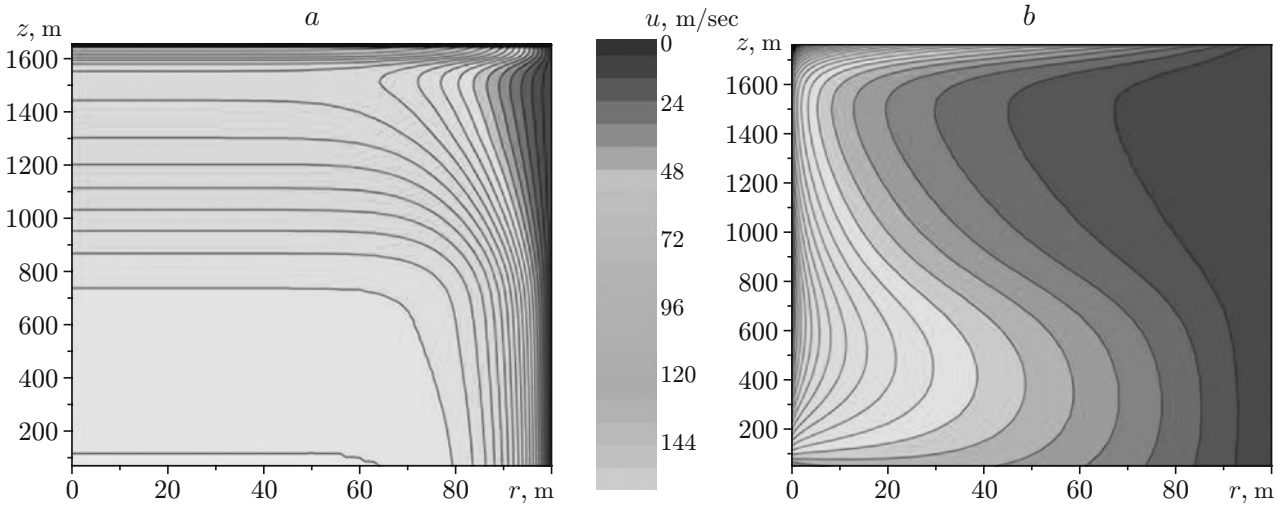

Fig. 2. Profiles of the boundary layers in the channel with the radius of 100 m: (a) $\mu = 10^5$ Pa · sec and $t = 3.5$ sec; (b) $\mu = 10^7$ Pa · sec and $t = 4$ sec.

2.1. *Case with Constant Melt Viscosity.* First we considered a simplified formulation of the unsteady problem, which implied that viscosity was constant over the column height and was not affected by liberation of the gas dissolved in the melt. The numerical analysis of boundary layer evolution was performed for three values of the constant melt viscosity: $\mu = 10^3$, 10^5, and 10^7 Pa · sec.

Figure 1a (the axis of symmetry on the left and the channel wall on the right) shows the flow structure in an ascending magma flow ($\mu = 10^3$ Pa · sec) formed by the time $t = 4$ sec in the volcano channel with the radius of 10 m. It is seen that the boundary layer approximately 0.5 m thick is formed on the wall; the mass velocity in this region is $u = 0$–8 m/sec. This range remains almost unchanged in the interval $H = 0$–800 m. When approaching the free surface, the boundary layer thickness increases and reaches the maximum value (1.5–2.0 m) at the height $H \approx 1500$ m. In an immediate vicinity of the free surface, the boundary layer thickness again decreases to 0.5 m.

Figure 1b shows the flow structure at $\mu = 10^5$ Pa · sec in the same channel at the time $t = 2$ sec. It is seen that the channel with the radius of 10 m is almost completely choked by the boundary layer if viscosity is increased by two orders of magnitude.

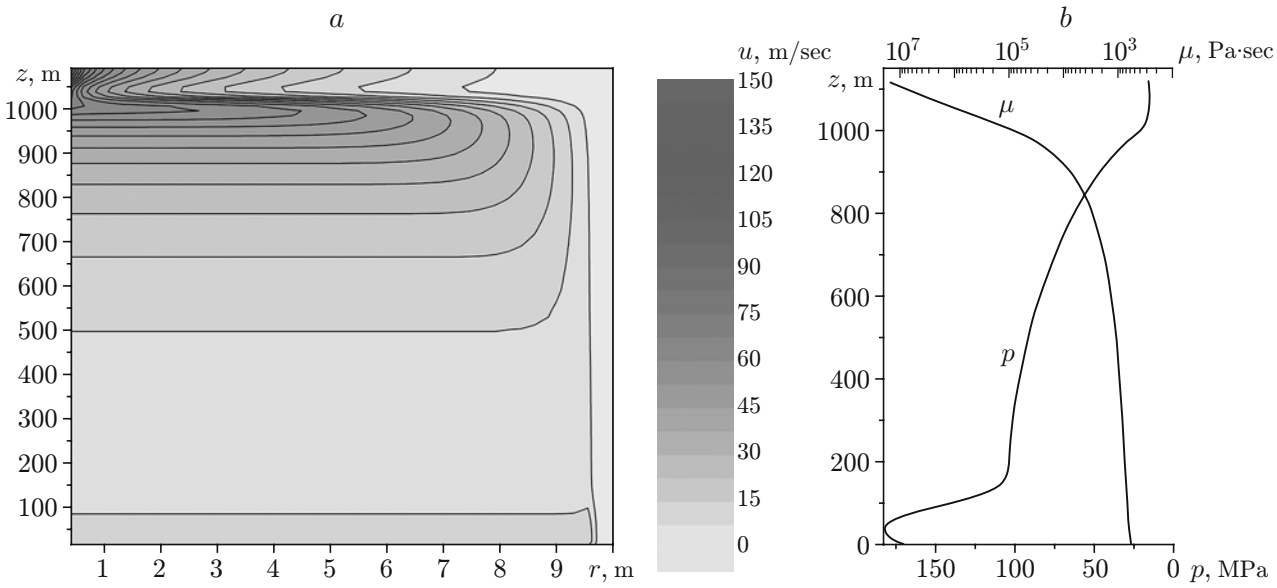

Fig. 3. Flow structure (a) and distributions of the pressure p in the decompression wave and of the viscosity μ along the magma column (b) at $t = 0.7$ sec.

The calculations illustrated in Fig. 2a predict the boundary layer formation on the channel wall in the magma flow with viscosity of 10^5 Pa $\cdot$ sec in the channel with the radius of 100 m. The thickness of the boundary layer "core" at the height $H = 1500$ m is approximately 15 m ($t = 3.5$ sec); the overall thickness can be approximately estimated as 30 m based on isoline configurations. As the melt viscosity is increased to $\mu = 10^7$ Pa $\cdot$ sec (Fig. 2b), the boundary layer at the same height penetrates over the channel width up to 70–80 m. At a distance of 50 m from the axis, the boundary layer occupies a significant part of the channel in the region between $H = 1700$ m and $H = 800$ m and squeezes the flow to the axis ($t = 4$ sec).

2.2. *Case with Dynamically Changing Viscosity.* A numerical analysis of the magma melt state dynamics with viscosity depending on the emergence of cavitating nuclei behind the decompression wave front and diffusion of the dissolved gas from the melt (Figs. 3 and 4) showed that the flow structure in this case is significantly different from that considered above (see Figs. 1 and 2). First of all, it should be noted that the magma melt viscosity near the volcanic chamber can be several orders smaller than that near the free surface. The viscosity distribution along the channel is time-dependent.

Figure 3a shows the flow structure formed by the time $t = 0.7$ sec, when the decompression wave front [curve $p(z)$ in Fig. 3b] propagates away from the free surface along the melt column and reaches the lower level (interface with the magma chamber) where a constant pressure is set. The pressure jump near this interface [curve $p(z)$ in Fig. 3b] and the increase in mass velocity up to $u = 40$ m/sec at a distance of 100 m from the interface show that the reflected wave is a compression wave.

The boundary layer formed by the time $t = 0.7$ sec is approximately 0.5 m thick at the height $H = 100$ m; its thickness linearly increases up to 0.7–0.8 m over the height from $H = 100$ m to $H = 1000$ m. A strong gradient is observed in the viscosity distribution near the free surface [curve $\mu(z)$ in Fig. 3b]: the viscosity increases by more than three orders of magnitude. Beginning from $H = 1000$ m, the boundary layer thickness drastically increases. The layer acquires the shape of some kind of a step on the channel wall and occupies a significant portion of its cross section, except for a small area with the radius of 2 m around the axis of symmetry, where the flow velocity is approximately 80 m/sec. The boundary layer penetrates along the magma column approximately by 50–70 m (at a distance of 5–6 m from the axis of symmetry), forming something like a "diaphragm."

Figure 3 reveals a feature, which is insignificant at first glance: dependence between the pressure jump in the interval $H = 0$–100 m and the boundary layer thickness, which decreases with increasing pressure. It follows from Fig. 4, which shows the flow structure formed by the time $t = 1.1$ sec and also the pressure and viscosity distributions, that this effect is not accidental. At $t = 1.1$ sec, the compression wave [jump on the curve $p(z)$] reflected from the

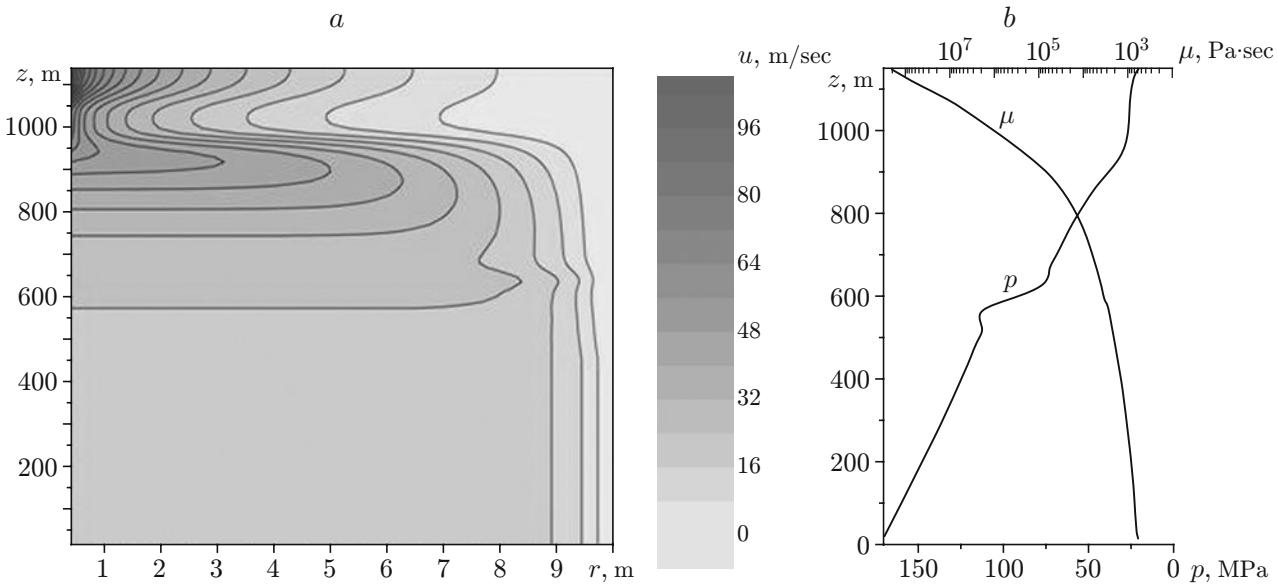

Fig. 4. Flow structure (a) and distributions of the pressure p and viscosity μ along the magma column (b) at $t = 1.1$ sec.

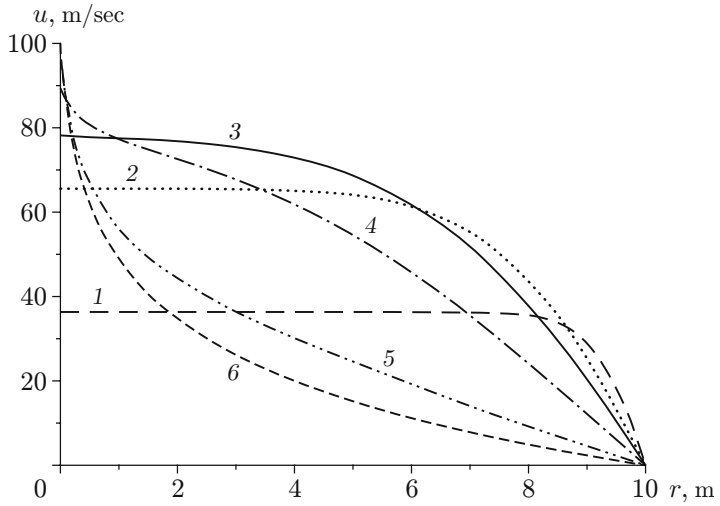

Fig. 5. Dynamics of the velocity profile in the middle cross section of the "diaphragm" of the magma channel at different times: $t = 0.3$ (1), 0.6 (2), 0.7 (3), 0.8 (4), 0.9 (5), and 1.1 sec (6).

lower boundary of the domain reaches the height $H = 600$ m (see Fig. 4b). It is seen in Fig. 4a that the boundary layer thickness substantially decreases at this height. The mechanism of this phenomenon is obvious: an increase in pressure in the reflected compression wave leads to a decrease in the degree of supersaturation of the magma by the dissolved gas, which results in a decrease in melt viscosity and, as a consequence, a local decrease in the boundary layer thickness.

It is also seen in Fig. 4 that the boundary layer thickness increases from 1.2 to 2 m during 0.4 sec in the range $H = 0$–900 m. At large heights, the flow pattern is actually similar to that shown in Fig. 3; it is only the scale of the characteristic structures that is changed: the boundary layer penetrates inward the melt channel almost by 200 m and forms a "diaphragm" overlapping approximately 70–80% (over the radius) of the cross-sectional area of the channel. At $H \approx 1000$ m, the melt flow is also concentrated near the axis of symmetry, and its velocity reaches 100 m/sec.

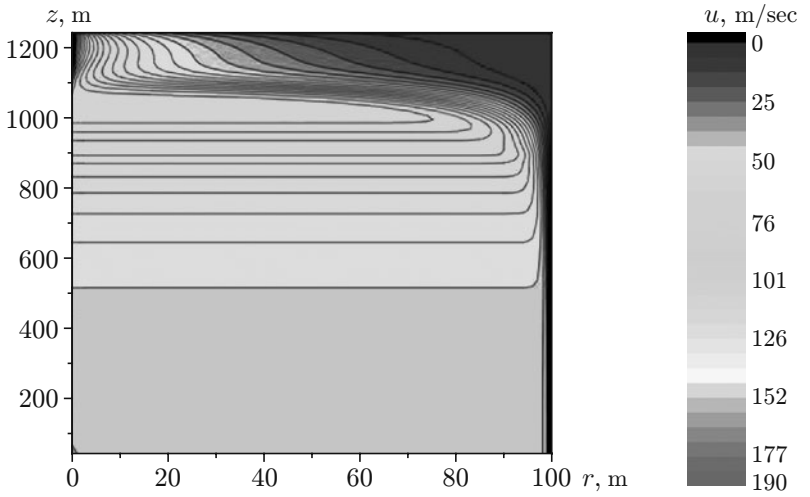

Fig. 6. Flow structure in the channel with the radius $r = 100$ m at $t = 1.4$ sec.

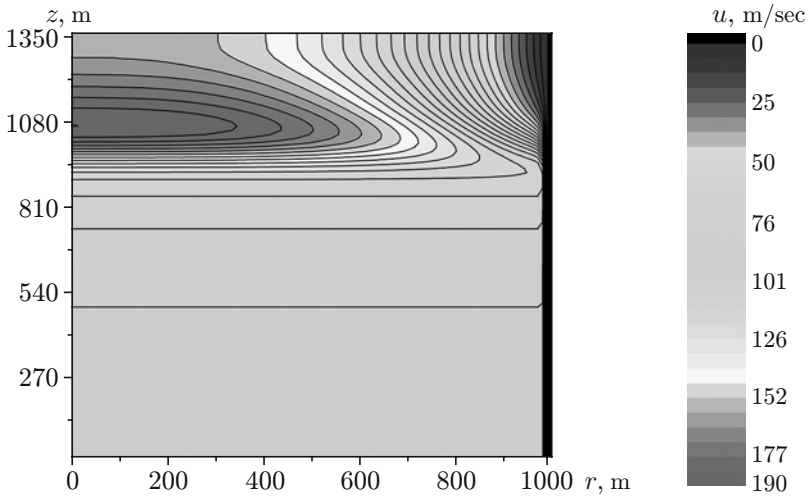

Fig. 7. Flow structure in the channel with the radius $r = 1000$ m at $t = 2$ sec.

The dynamics of the velocity profile in the cross section of the "diaphragm" overlapping the channel cross section (see Figs. 3 and 4) is illustrated in Fig. 5. The initially classical velocity profile (curve 1) almost completely changes its character by the time $t = 0.8$ sec (curve 4) as the cavitation processes develop owing to diffusion of the gas dissolved in the melt to cavitating bubbles and a rapid increase in viscosity. At $t = 1.1$ sec, the flow is localized in a narrow area around the axis of symmetry (curves 5 and 6 in Fig. 5).

An analysis of results calculated for the channel with the radius of 10 m allows us to conclude that further constriction of the channel is possible, up to its complete choking. This assumption is confirmed by results of studying the boundary layer evolution in channels with the radii of 100, 500, and 1000 m (Figs. 6 and 7). In particular, an analysis of the flow structure dynamics in the channel with the radius of 100 m showed that there is a specific feature in the boundary layer development behind the front of the decompression wave propagating over the magma column, which is observed already at the initial stage of wave propagation: beginning from the value $H \approx 1000$ m, the boundary layer rapidly grows toward the axis, simultaneously capturing the upper part of the column where cavitation is intensely developing. The boundary layer formation in the channel cross section is almost completed by the time $t = 0.75$ sec. The boundary layer occupies a substantial portion of the channel cross section, while the thickness of the "diaphragm" (approximately equal to 40 m) with the inner radius near the axis of symmetry equal to 20–30 m increases with time and reaches approximately 150 m by the time $t = 1.4$ sec (Fig. 6).

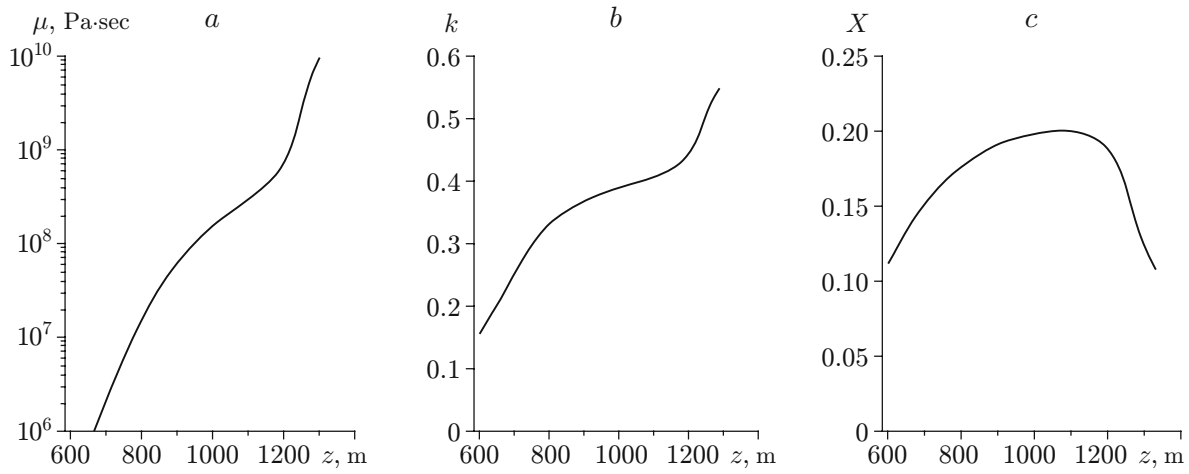

Fig. 8. Distributions of viscosity (a) and volume fractions of the gaseous (b) and crystalline (c) phases along the z axis at the time $t = 2.1$ sec.

The channel structure is unchanged with a further increase in the channel radius: the boundary layer grows predominantly in the upper part of the magma column, the flow is squeezed to the axis of symmetry, and the flow velocity increases (see Fig. 7). In channels with the radii of 500 and 1000 m, the boundary layer structure testifies to the explosive character of its evolution: the boundary layer has an approximately constant thickness at the height $H = 0$–1000 m, which drastically increases to 150 m at $H = 1080$–1350 m. The explosive character of the boundary layer evolution can be explained by comparing the distributions of the basic characteristics of the three-phase magma (Fig. 8) [17]. Correlations between the intense growth of melt viscosity (almost by two orders), the drastic increase in the volume fraction of the gas phase, and the decrease in the volume fraction of the crystalline phase are clearly visible in Fig. 8. As the nucleation process in the upper part of the magma column is finalized long before the time instant considered, the jump of the function k can be attributed, apparently, only to the "ejection" of a significant mass of the gas dissolved in the magma to cavitating bubbles. The loss of the gas causes the increase in viscosity and, as a consequence, the explosive character of boundary layer formation.

Conclusions. A numerical analysis of the dynamics of the field of mass velocities of the viscous magma shows that the boundary layer can form on the volcano channel walls; intense evolution of the boundary layer together with a strong gradient of the boundary layer thickness over the magma column height is responsible for the effect of channel choking.

With an increase in viscosity from $\mu = 10^3$ to $\mu = 10^5$ and 10^7 Pa $\cdot$ sec, the characteristic thickness of the boundary layer becomes comparable with the channel radius. In particular, channels with the radii of 10 m ($\mu = 10^5$ Pa $\cdot$ sec) and 100 m ($\mu = 10^7$ Pa $\cdot$ sec) are almost completely overlapped by the boundary layer over the entire channel height; the flow is squeezed by the boundary layer in a narrow zone around the axis of symmetry.

The flow structure is substantially different if the viscosity due to the emergence of cavitating nuclei and diffusion of the gas dissolved in the melt away from the latter are taken into account. In the channel with the radius of 10 m, the boundary layer occupies a significant portion of the cross-sectional area of the channel at the height $H \approx 1000$ m (approximately 70–80% over the radius) and penetrates inward the melt column approximately by 200 m. The boundary layer acquires a clearly expressed structure similar to a "diaphragm," which squeezes the cavitating magma flow in a bounded channel with the radius of 2–3 m. The melt flow velocity in this channel near the axis of symmetry increases to 100 m/sec.

The results presented in the paper allow us to assume that the intense growth of boundary layers occupying a significant portion of the cross-sectional area of the volcanic channel can be considered as one possible mechanism responsible for periodicity (cyclicity) of ejections having an explosive character during the volcanic eruption.

This work was supported by the Russian Foundation for Basic Research (Grant No. 09-01-00500-a), by the Integration Project No. 12.12 of the Presidium of the Russian Academy of Sciences, and by the Integration Project No. 59 of the Siberian Division of the Russian Academy of Sciences.

REFERENCES

1. H. M. Gonnermann and M. Manga, "The fluid mechanics inside a volcano," *Annu. Rev. Fluid Mech.*, **39**, 321–356 (2007).
2. C. Jaupart and S. Vergniolle, "Laboratory models of hawaiian and strombolian eruptions," *Nature*, **331**, 58–60 (1988).
3. E. A. Parfitt, "A discussion of the mechanisms of explosive basaltic eruptions," *J. Volcanol. Geotherm. Res.*, **134**, 77–107 (2004).
4. E. A. Blackburn, L. Wilson, and S. Sparks, "Mechanism and dynamics of strombolian activity," *J. Geol. Soc. London*, **132**, 429–440 (1976).
5. L. Wilson, "Relationships between pressure, volatile content and eject a velocity in three types of volcanic explosion," *J. Volcanol. Geotherm. Res.*, **8**, 297–313 (1980).
6. V. K. Kedrinskii, A. I. Makarov, S. V. Stebnovskii, and K. Takayama, "Explosive eruption of volcanoes: some approaches to simulation," *Combust., Expl., Shock Waves*, **41**, No. 6, 777–786 (2005).
7. V. K. Kedrinskii and A. I. Makarov, "Dynamics of cavitating magma state at explosive eruption," in: *Proc. of the 6th Int. Symp. on Cavitation* (CAV2006) (Wageningen, Netherlands, September 11–15, 2006), Maritime Res. Inst. Netherlands, Wageningen (2006), Paper No. 167, pp. 1–8.
8. S. Vergniolle and C. Jaupart, "Dynamics of degassing at Kilauea volcano, Hawaii," *J. Geophys. Res.*, **95**, 2793–2809 (1990).
9. D. A. Swanson and R. T. Holcomb, "Regularities in growth of the Mount St. Helens dacite dome 1980–1986," in: J. H. Fink (ed.), *Lave Flows and Domes: Emplacement Mechanisms and Hazard Implications*, Springer Verlag, Berlin (1990), pp. 3–24.
10. B. Voight, S. Sparks, A. D. Miller, et al., "Magma flow instability and cyclic activity at Soufriere Hills Volcano, Montserrat, British West Indies," *Science*, **283**, 1138–1142 (1999).
11. V. K. Kedrinskii, "Explosive eruptions of volcanoes: simulation, shock tube methods and multi-phase mathematical models (plenary lecture)," in: *Proc. of the 26th Int. Symp. on Shock Waves* (Goettingen, Germany, July 17–21, 2007), Vol. 1, Springer Verlag, Berlin–Heidelberg (2009), pp. 19–26.
12. R. P. Denlinger and R. P. Hobitt, "Cyclic eruptive behavior of silicic volcanoes," *Geology*, **27**, 459–462 (1999).
13. A. Barmin, O. Melnic, and S. Sparks, "Periodic behavior in lava dome eruptions," *Earth. Planet. Sci. Lett.*, **199**, 173–184 (2002).
14. K. L. Mitchel, "Coupled conduit flow and shape in explosive volcanic eruptions," *J. Volcanol. Geotherm. Res.*, **143**, 187–203 (2005).
15. A. M. Rubin, "Propagation of magma-filled cracks," *Annu. Rev. Earth Planet. Sci.*, **23**, 287–336 (1995).
16. A. Gerst, M. Hort, P. R. Kyle, and M. Voege, "The first second of a strombolian eruption: velocity observations at Erebus volcano, Antarctica," *EOS, Trans. Am. Geophys. Union*, **87**, No. 52 (2005), Fall Meet. Suppl. Abstr. V31G-04.
17. V. K. Kedrinskii, M. N. Davydov, A. A. Chernov, and K. Takayama, "Initial stage of the explosive eruption of volcanoes: magma state dynamics in unloading waves," *Dokl. Ross. Akad. Nauk*, **407**, No. 2, 190–193 (2006).
18. V. K. Kedrinskii, M. N. Davydov, A. A. Chernov, and K. Takayama, "Generation and evolution of cavitation in magma under dynamic unloading," *J. Appl. Mech. Tech. Phys.*, **46**, No. 2, 208–215 (2005).
19. E. S. Persikov, "The viscosity of magmatic liquids: experiment, generalized patterns. A model for calculation and prediction. Applications," in: *Physical Chemistry of Magmas*, Vol. 9: *Advances in Physical Geochemistry*, Springer Verlag, New York (1991), pp. 1–40.
20. V. K. Kedrinskii and S. Plaksin, "Rarefaction wave structure in a cavitating liquid," in: *Proc. of the 11th Symp. on Nonlinear Acoustics* (Novosibirsk, August 24–28, 1987), Vol. 1, Sib. Branch USSR Acad. Sci. (1987), pp. 51–55.